

SCIENTIFIC REPORTS

OPEN

Origin of multiple band gap values in single width nanoribbons

Deepika¹, Shailesh Kumar², Alok Shukla^{3,†} & Rakesh Kumar¹

Received: 27 June 2016
Accepted: 07 October 2016
Published: 03 November 2016

Deterministic band gap in quasi-one-dimensional nanoribbons is prerequisite for their integrated functionalities in high performance molecular-electronics based devices. However, multiple band gaps commonly observed in graphene nanoribbons of the same width, fabricated in same slot of experiments, remain unresolved, and raise a critical concern over scalable production of pristine and/or hetero-structure nanoribbons with deterministic properties and functionalities for plethora of applications. Here, we show that a modification in the depth of potential wells in the periodic direction of a supercell on relative shifting of passivating atoms at the edges is the origin of multiple band gap values in nanoribbons of the same width in a crystallographic orientation, although they carry practically the same ground state energy. The results are similar when calculations are extended from planar graphene to buckled silicene nanoribbons. Thus, the findings facilitate tuning of the electronic properties of quasi-one-dimensional materials such as bio-molecular chains, organic and inorganic nanoribbons by performing edge engineering.

Quasi-one-dimensional nanoribbons in their sub-10 nm width are focus of current research interest amongst low dimensional materials due to their exceptional promises to enable new functionalities, and improve the performance of devices down to molecular level^{1–5}. Nevertheless, band gap of graphene nanoribbons (GNRs)^{6–8} is critical in addition to its other interesting electronic properties such as quasi-relativistic behavior of charge carriers⁹, the highest thermal conductivity¹⁰, and the highest mobility¹¹ of charge carriers at room temperature for such high performance applications^{12,13}. The common experimental observations of multiple band gaps due to different passivation patterns at the edges in graphene nanoribbons (GNRs) of the same width have been neglected so far, since the focus of research on GNRs has been to understand the experimental observation of non-zero band gap values in both the crystallographic orientations. Multiple band gaps were observed in GNRs of the same width fabricated even in the first experiment performed on GNRs in 2007¹⁴. Later, several experimental papers also reported multiple band gap values corresponding to different passivation patterns at the edges in GNRs of the same width and other quasi-one dimensional materials such as silicon nanowires fabricated in a crystallographic orientation^{15–20}. Since 2007, hundreds of theoretical papers have been published on GNRs focusing only on how to explain non-zero band gap in both the crystallographic orientations of GNRs based on different edge passivating patterns with different type of edge passivating elements^{21–28}, the multiple band gap values in nanoribbons of the same width remains unresolved. Therefore, in this work, we for the first time propose a resolution for the physical origin of multiple band gap values in single width nanoribbons, which would resolve the critical concern over the scalable production of pristine and/or hetero-structure nanoribbons with deterministic properties for plethora of applications.

For theoretical investigation of the multiple band gaps in nanoribbons of the same width, we consider supercells in a crystallographic orientation with the same number of atoms. The supercells are different only in terms of arrangement of atoms at the edges with respect to each other. We have chosen oxygen as passivating atoms at the edges of nanoribbons because oxygen plasma is commonly used in fabrication of GNRs. The considered supercell edge configurations of GNRs are energetically favorable with respect to other possible edge configurations having the same number of atoms in a crystallographic orientation (*cf.* Supplementary Information S1). Band structure calculations show an appreciable change in the band gap values in nanoribbons of the same width, however their ground state energy are practically the same. Based on theoretical analysis, it is found that the modification in the Columbic potential profiles in the periodic direction is the origin of multiple band gap values in the fabricated

¹Department of Physics, Indian Institute of Technology Ropar, Rupnagar-140001, India. ²School of Chemistry, Physics and Mechanical Engineering, Queensland University of Technology, Brisbane, Queensland 4000, Australia. ³Department of Physics, Indian Institute of Technology Bombay, Powai, Mumbai-400076, India. [†]Present address: Physics Department, Bennett University, Plot No. 8–11, Techzone II, Greater Noida 201310 (UP), India. Correspondence and requests for materials should be addressed to R.K. (email: rakesh@iitrpr.ac.in)

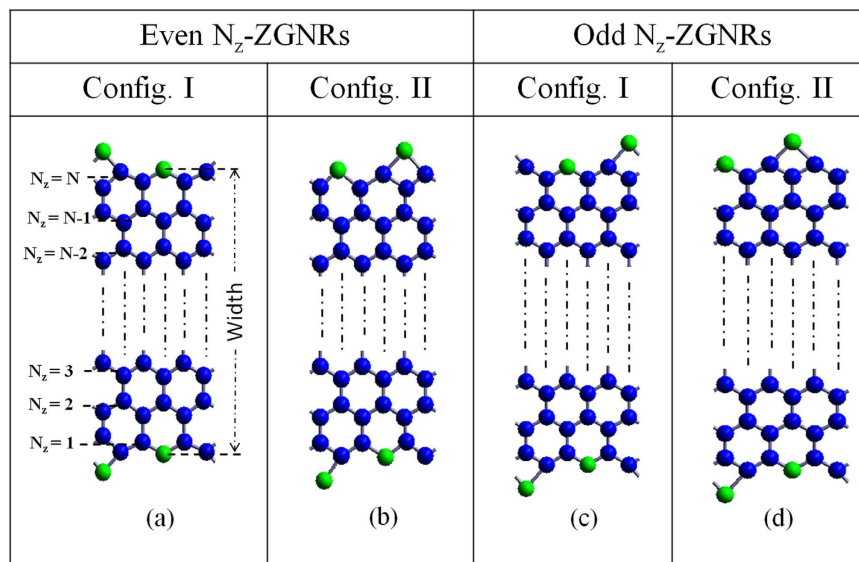


Figure 1. Two possible edge configurations for ZGNRs supercell, (a,b) represents configurations corresponding to even N_z -ZGNRs, while (c,d) corresponds to odd N_z -ZGNRs. Blue and green spheres represent carbon and oxygen atoms, respectively. Note: In both configurations, the bottom edge remains the same, only the relative arrangement of atoms on the top edge is different.

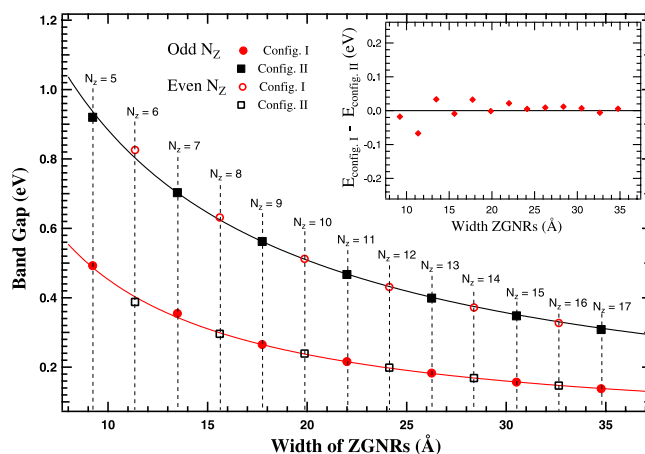


Figure 2. Energy band gap values as a function of width corresponding to configurations I and II of ZGNRs. Solid curves show fitting to the band gap values using scaling formula $\Delta E = \frac{\alpha}{(w + w')}$ for GNRs, where ΔE is the band gap (eV), α (eV.Å) is the scaling factor, and $w + w'$ (Å) is the equivalent width of nanoribbons. Dotted vertical lines are drawn to represent two band gap values for ZGNRs of the same width. Inset figure shows the difference of the ground state energy values for config. I and config. II as a function of width for ZGNRs.

GNRs. The results are verified when calculations are extended from planar graphene nanoribbons to buckled silicene nanoribbons (SiNRs), GNRs passivated with multiple functional groups at the edges, and rough edged GNRs. Thus, the findings facilitate in tuning the electronic properties of quasi-one-dimensional materials such as bio-molecular chains, organic and inorganic nanoribbons by edge engineering, which improve the performance of devices down to molecular level for their wide applications^{29–33}.

Results and Discussions

To investigate the origin of multiple band gaps in nanoribbons of the same width in a crystallographic orientation, we consider GNRs with two edge configurations (config. I and config. II). For ZGNRs, two edge configurations (I and II) for supercells corresponding to even N_z and odd N_z are shown in Fig. 1. Band structures are calculated from Γ ($k=0$) to X-point ($k=\pi$) upto a maximum width of ≈ 35 Å ($N_z = 17$). Typical band structures for $N_z = 5$ and 6-ZGNRs of config. I and config. II are shown in Supplementary Information S2. Non-zero direct band gaps are observed at Γ point for both the configurations. An appreciable difference in the band gap values are observed in ZGNRs of the same width (Fig. 2). The difference in the band gap values decreases with increase in the width of ZGNRs. It is to be noted that even after having significant change in the band gap values in ZGNRs of the same

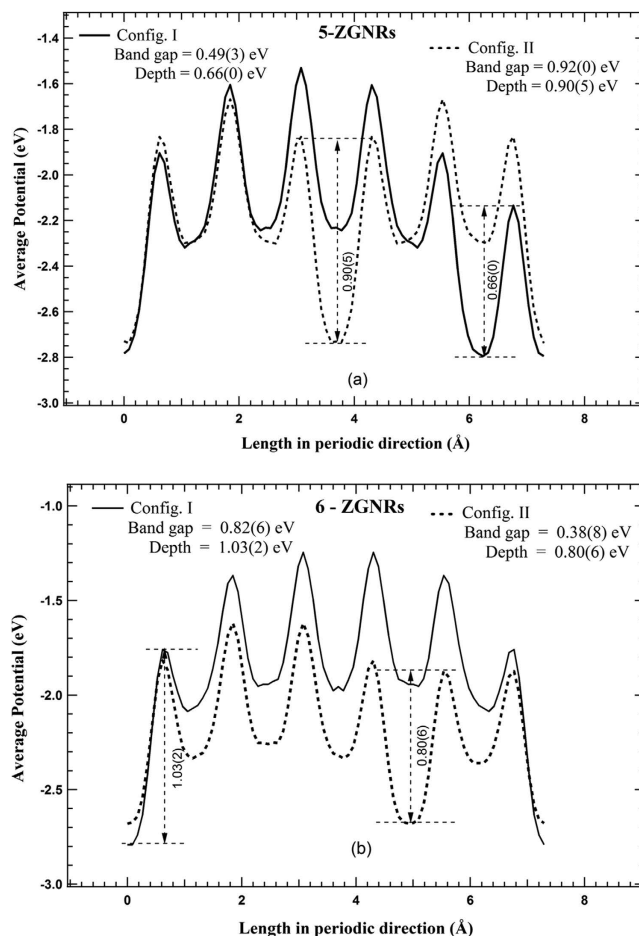


Figure 3. Average of the local potentials of YZ atomic plane plotted in periodic direction of the supercell for (a) 5-ZGNRs and (b) 6-ZGNRs. Note: Switching of the deepest potential well and band gap values from config. II ($N_z=5$) to config. I ($N_z=6$).

width, their ground state energies remain practically the same (inset of Fig. 2). The maximum difference in the ground state energy is $\approx 0.06(6)$ eV for $N_z=6$, which further decreases with the width. Electrostatic edge-edge interactions are one possible reason behind the small difference in the ground state energies of both the configurations. To explore this possibility further, we placed discrete electronic charges on the atomic sites at the edges, and calculated the difference of the electrostatic energy for the two configurations. This energy difference, although a bit larger, is of the same order of magnitude as compared to the difference between the ground state energies of both the configurations for nanoribbons of the same width. This result suggests the Coulombic nature of the edge-edge interactions, and relates the change in the ground state energy with the modification in the potential energy as a consequence of change in the arrangement of atoms at the edges.

Since one dimensional periodic potential is the limiting case for the periodic potential of a quasi-one-dimensional nanoribbons, therefore an average of the local potentials along the width of the nanoribbon projected on periodic direction may be considered to explain the difference in the band gap values. In order to investigate it, we plotted potential profiles (average of local potentials in the periodic direction) of the ZGNRs supercells, which looks similar to that of Kronig-Penney (KP) potential wells. Typical potential profiles corresponding to config. I and config. II for both $N_z=5$ and 6 are shown in Fig. 3. The number of potential wells in a supercell along the periodic direction is equal to that of the atomic YZ planes, and a change in potential profiles corresponding to config. I and config. II for ZGNRs of the same width is observed [Fig. 3(a,b)]. From KP model, for the same width of potential wells, the band gap is proportional to the depth of well. Therefore, the depth of the deepest potential well at global minimum is compared for both the configurations. The configuration with the deepest well at global minimum amongst the potential wells is found to have higher band gap value in agreement with the theory of KP model. The normalized potential depth of the deepest well at global minimum (w.r.t. N_z) is plotted as a function of width for the config. I and config. II for ZGNRs (Fig. 4). It is to be noted that as N_z is changed to N_{z+1} , the deepest potential well switches from one configuration to another configuration, and accordingly higher band gap value also switches to another configuration (Figs 2 and 4). This explains a change in the depth of the deepest well at global minimum in potential profile of a supercell, resulting from a change in the arrangement of atoms at the edges, to be the origin of multiple band gap values for the same width of ZGNRs. The difference in the band gap values decreases similar to that of the average normalized potentials for higher widths of ZGNRs (Fig. 4), which

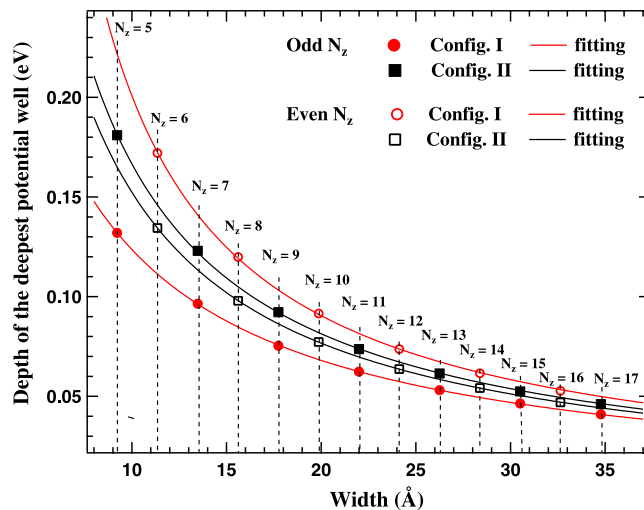


Figure 4. The normalized depth of the deepest potential well (w.r.t. N_z) plotted as a function of width for config. I and config. II of ZGNRs. Solid curves correspond fitting to the scaling formula same as that for band gap values (see caption of Fig. 2).

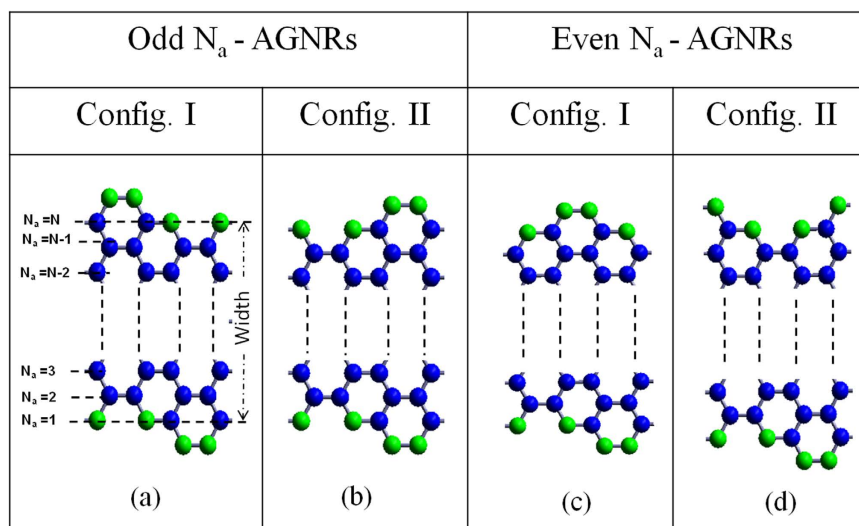


Figure 5. Two possible edge configurations for AGNRs supercell corresponding to odd N_a [(a,b)] and even N_a [(c,d)]. Blue and green spheres represent carbon and oxygen atoms, respectively. Note: Change in relative arrangement of atoms at edges in config. I and config. II.

indicates the decreasing edge effects on the average of local potentials in higher widths of ZGNRs. Therefore, the effect of a change in the potential profile on the band gap is primarily a consequence of modification in the electrostatic interactions among the charges at the edges of nanoribbons.

For investigating the effect of potential profiles on band gap in armchair GNRs, two edge configurations for N_a -AGNRs are considered similar to that of ZGNRs. Two edge configurations for AGNRs supercell of odd N_a and even N_a are shown in Fig. 5. Band structures are calculated up to a maximum width of $\approx 23 \text{ \AA}$ ($N_a = 20$). Typical band structures for $N_a = 5$ and 6-AGNRs of config. I and config. II are shown in Supplementary Information S3. Direct band gap is observed at Γ ($k = 0$) point for both the configurations. It is to be noted that the multiple band gap values are observed only for odd N_a -AGNRs, while the same band gap values are observed for even N_a -AGNRs. The difference in band gap values between both the configurations of odd N_a -AGNRs decreases with the increase in the width. The ground state energy corresponding to both the configurations of AGNRs are nearly same (negligible change in the third decimal place) for supercells of the same width, except for $N_a = 5$ and 7. The exceptional behavior for $N_a = 5$ and 7-AGNRs has been discussed in Supplementary Information S4.

Similar to ZGNRs, potential profiles of AGNRs are plotted for both the configurations in periodic direction of the supercells. For odd N_a -AGNRs, the edge configuration with the deepest potential well at global minimum corresponds to the higher band gap value except for $N_a = 5$ and 7. For even N_a -AGNRs, the potential profiles of both the configurations superpose on each other on relative shifting in the periodic direction as shown in Fig. 6.

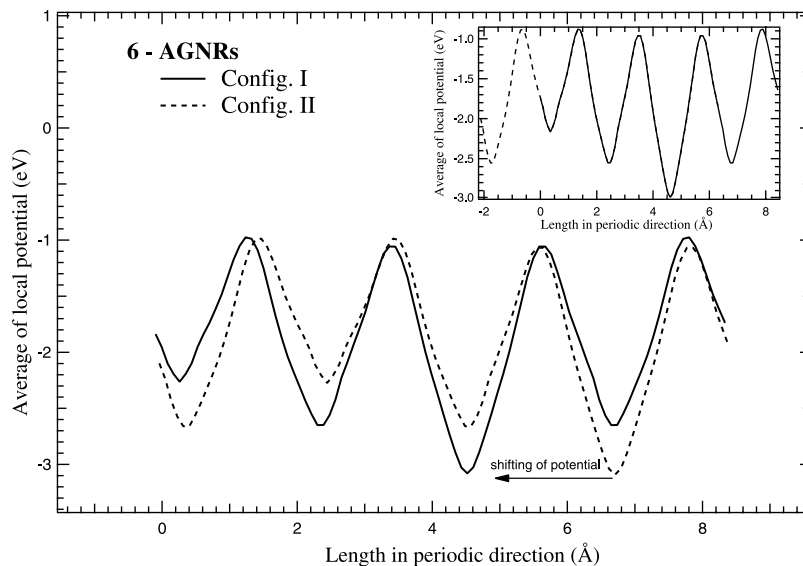


Figure 6. The average of local potentials plotted along the periodic direction of 6-AGNRs supercell. Inset shows the superposition of the potential profiles on a relative shifting of config. II w.r.t. config. I.

Therefore, both the configurations of even N_a -AGNRs correspond to the same band gap values, while different band gap values are observed for odd N_a -AGNRs. The difference in the band gap values of both the configurations for odd N_a -AGNRs becomes negligible for $N_a = 15$ onwards. Nevertheless, a small but nearly constant difference between the deepest potential wells at global minimum of the configurations for higher widths is observed possibly as a consequence of inherent potential associated with the configurations.

To summarize, multiple band gap values in GNRs of the same width in a crystallographic orientation depends upon the relative arrangement of atoms at the edges in the supercells. On changing the arrangement of atoms at the edges, band gap is changed only for an asymmetrical modification in potential profiles of the supercells. Band gap is found to be higher for a configuration with the deepest potential well at the global minimum amongst GNRs of the same width. How fast the difference in the band gap values between both the configurations of GNRs would decrease, depends upon arrangement of atoms at the edges in a supercell.

To generalize the concept for multiple band gaps in nanoribbons of the same width, we apply configurational change at the edges to buckled silicene nanoribbons of the same width (*cf.* Supplementary Information S5) as it is done for GNRs. In the case of silicene, oxygen passivated zigzag configuration similar to ZGNRs is theoretically not possible due to higher value of Si-Si bond lengths ≈ 2.23 Å (lattice constant for silicene lattice ≈ 3.826 Å) in comparison to Si-O bond length of ≈ 1.538 Å. Therefore, the studies are carried only for armchair silicene nanoribbons (ASiNRs). The results are similar to GNRs. Multiple band gap values are observed on changing the arrangement of atoms at the edges for the same width of odd N_a -ASiNRs, and no difference is observed for even N_a -ASiNRs. Higher band gap value corresponds to the configuration with the deepest potential well at global minimum except for $N_a = 5$ and 7. The exceptional behavior for $N_a = 5$ and 7 is found to be the same as that for $N_a = 5$ and 7-AGNRs. The difference in the band gap values between both configurations of SiNRs decreases with width similar to GNRs, which reflects the decreasing edge-contributions to the potential profiles in higher width of nanoribbons.

In order to verify the concept of multiple band gaps for nanoribbons passivated with different types of atoms at the edges, such as bio-molecular chains passivated with different group of elements at the edges, we consider GNRs passivated with two different types of atoms such as hydrogen and oxygen. Similar to the above findings, multiple band gap values are observed for GNRs of the same width with practically the same ground state energy (*cf.* Supplementary Information S6). The effect of a change in the arrangement of atoms at the edges is also observed on band gaps in rough edged GNRs passivated with oxygen atoms; a significant change in the band gap values are observed for rough edged GNRs of the same width with practically the same ground state energy (*cf.* Supplementary Information S7). The finding is relevant for explanation of the experimental observations of multiple band gap values in GNRs of the same width fabricated in a crystallographic orientation using oxygen plasma etching process.

Conclusions

On the basis of our first-principles calculations, it is concluded that

- Origin of multiple band gap values in nanoribbons of the same width, same crystallographic orientation, and the same number of the atoms in the supercells is a consequence of modification in the potential profile in the periodic direction, although they have practically the same ground state energy.

- The modification in the depth of the potential well is primarily a consequence of change in the electrostatic interactions among the charges at the edges of nanoribbons, which arise from a change in the arrangement of atoms at the edges.
- Asymmetrical modification in the potential profiles results into a significant change in the band gap value of a nanoribbon, while symmetrical modification leads to the same band gap values.
- The configuration with the deepest potential well at the global minimum in the potential profile of a supercell corresponds to the highest band gap value of a nanoribbon except for the supercells having modifications in the bond lengths on a change in the arrangement of atoms at the edges.
- The difference in the band gap values of both the configurations decreases with increase in width of nanoribbons, which indicates decreasing edge effects on the potential profiles, therefore would converge at higher width. How fast it would converge depends typically on arrangement of atoms at the edges.

As a final remark, we would like to state that it is possible to obtain multiple band gaps in nanoribbons of the same width, by changing the relative arrangement of atoms at the edges in nanoribbons of the same width. The concept can be applied to understand the experimental observations of multiple band gap values in nanoribbons of the same width, and also the physical origin of the differential behavior in bio-molecules such as protein and carbohydrates, where only the relative position of the molecular functional group changes at the edges. These findings are critical for edge engineering of quasi-one-dimensional materials and bio-molecules. With deterministic control at the edges, the properties of quasi-one-dimensional materials and bio-molecules can be tuned for designing new biomaterials³⁴, leading to molecular level solution to the problems related to environment, food industry, biotechnology and medicines.

Methods

We performed first-principles band structure calculations for nanoribbons based on density functional theory (DFT) using Vienna *ab-initio* simulation package (VASP)³⁵. Generalized gradient approximations are used as exchange-correlation functional with electron-ion interactions in projected augmented wave formalism. The cutoff energy of 400 eV and 800 eV is used for graphene and silicene, respectively with a vacuum layer of ≈ 10 Å. The relaxation of the system is performed until the force experienced by each atom is ≤ 0.001 eV. Å⁻¹. The Monkhorst-Pack k-space mesh of $25 \times 1 \times 1$ is used for the k-space sampling. All the calculations for nanoribbons are performed for nonmagnetic ground state, since the ground state is found to be nonmagnetic upon introducing spin-polarization. Number of zigzag chains or dimer lines along normal to the periodic direction is used to represent the width of the nanoribbons, and higher width of nanoribbons is obtained by adding pure carbon chains or dimer lines. The number of zigzag chains (N_z) for zigzag graphene nanoribbons (ZGNRs) corresponds to N_z -ZGNRs and number of dimer lines (N_a) for armchair graphene nanoribbons (AGNRs) as N_a -AGNRs; and the similar nomenclature is applied to SiNRs.

References

1. van der Lit, J. *et al.* Suppression of electron-vibron coupling in graphene nanoribbons contacted via a single atom. *Nature Commun.* **4**, 2023 (2013).
2. Welte, L., Calzolari, A., Di Felice, R., Zamora, F. & Gómez-Herrero, J. Highly conductive self-assembled nanoribbons of coordination polymers. *Nature Nanotech.* **5**, 110 (2010).
3. Zhong, Y. *et al.* Helical Ribbons for Molecular Electronics. *J. Am. Chem. Soc.* **136**, 8122 (2014).
4. Cai, J. *et al.* Atomically precise bottom-up fabrication of graphene nanoribbons. *Nature* **466**, 470 (2010).
5. Gracia-Espino, E. *et al.* Fabrication of One-Dimensional Zigzag [6,6]-Phenyl-C61-Butyric Acid Methyl Ester Nanoribbons from Two-Dimensional Nanosheets. *ACS Nano* **9**, 10516 (2015).
6. Wallace, P. R. The Band Theory of Graphite. *Phys. Rev.* **71**, 622 (1947).
7. Nakada, K., Fujita, M., Dresselhaus, G. & Dresselhaus, M. S. Edge state in graphene ribbons: Nanometer size effect and edge shape dependence. *Phys. Rev. B* **54**, 17954 (1996).
8. Son, Y.-W., Cohen, M. L. & Louie, S. G. Energy Gaps in Graphene Nanoribbons. *Phys. Rev. Lett.* **97**, 216803 (2006).
9. Novoselov, K. S. *et al.* Two-dimensional gas of massless Dirac fermions in graphene. *Nature* **438**, 197 (2005).
10. Balandin, A. A. *et al.* Superior Thermal Conductivity of Single-Layer Graphene. *Nano Lett.* **8**, 902 (2008).
11. Bolotin, K. I., Sikes, K. J., Hone, J., Stormer, H. L. & Kim, P. Temperature-Dependent Transport in Suspended Graphene. *Phys. Rev. Lett.* **101**, 096802 (2008).
12. Novoselov, K. S. *et al.* A roadmap for graphene. *Nature* **490**, 192 (2012).
13. Geim, A. K. & Novoselov, K. S. The rise of graphene. *Nature Materials* **6**, 183 (2007).
14. Han, M. Y., Özyilmaz, B., Zhang, Y. & Kim, P. Energy Band-Gap Engineering of Graphene Nanoribbons. *Phys. Rev. Lett.* **98**, 206805 (2007).
15. Li, X., Wang, X., Zhang, L., Lee, S. & Dai, H. Chemically Derived, Ultrasmooth Graphene Nanoribbon Semiconductors. *Science* **319**, 1229 (2008).
16. Zhu, Y. F., Dai, Q. Q., Zhao, M. & Jiang, Q. Physicochemical insight into gap openings in graphene. *Scientific Reports* **3** (2013).
17. Tseng, F., Unluer, D., Holcomb, K., Stan, M. R. & Ghosh, A. W. Diluted chirality dependence in edge rough graphene nanoribbon field-effect transistors. *Appl. Phys. Lett.* **94**, 223112 (2009).
18. Molitor, F. *et al.* Energy and transport gaps in etched graphene nanoribbons. *Semicond. Sci. Technol.* **25**, 034002 (2010).
19. Schwierz, F. Graphene transistors. *Nature Nanotech.* **5**, 487 (2010).
20. Mohammad, N. S. Understanding quantum confinement in nanowires: basics, applications and possible laws. *J. Phys.: Condens. Matter* **26**, 423202 (2014).
21. Sols, F., Guinea, F. & Neto, A. H. C. Coulomb Blockade in Graphene Nanoribbons. *Phys. Rev. Lett.* **99**, 166803 (2007).
22. Liao, T. *et al.* Charge carrier exchange at chemically modified graphene edges: a density functional theory study. *J. Mater. Chem.* **22**, 8321 (2012).
23. Hod, O., Peralta, J. E. & Scuseria, G. E. Edge effects in finite elongated graphene nanoribbons. *Phys. Rev. B* **76**, 233401 (2007).
24. Cruz-Silva, E. *et al.* Edge-Edge Interactions in Stacked Graphene Nanoplatelets. *ACS Nano* **7**, 2834 (2013).
25. Lee, G. & Cho, K. Electronic structures of zigzag graphene nanoribbons with edge hydrogenation and oxidation. *Phys. Rev. B* **79**, 165440 (2009).

26. Ramasubramaniam, A. Electronic structure of oxygen-terminated zigzag graphene nanoribbons: A hybrid density functional theory study. *Phys. Rev. B* **81**, 245413 (2010).
27. Liu, J. *et al.* Toward Cove-Edged Low Band Gap Graphene Nanoribbons. *J. Am. Chem. Soc.* **137**, 6097 (2015).
28. Deepika, Kumar, T. J. D., Shukla, A. & Kumar, R. Edge configurational effect on band gaps in graphene nanoribbons. *Phys. Rev. B* **91**, 115428 (2015).
29. Lemme, M. C., Echtermeyer, T., Baus, M. & Kurz, H. A Graphene Field-Effect Device. *IEEE Electron Device Letters* **28**, 282 (2007).
30. Pumera, M. Graphene in biosensing. *Materials Today* **14**, 308 (2011).
31. Shukla, A., Kumar, R., Mazher, J. & Balan, A. Graphene made easy: High quality, large-area samples. *Solid State Communications* **149**, 718 (2009).
32. Nair, R. R. *et al.* Fine structure constant defines visual transparency of graphene. *Science* **320**, 1308 (2008).
33. Yoon, Y. & Salahuddin, S. Dissipative transport in rough edge graphene nanoribbon tunnel transistors. *Appl. Phys. Lett.* **101**, 263501 (2012).
34. Rouge, J. L., Eaton, B. E. & Feldheim, D. L. Biomolecules in the synthesis and assembly of materials for energy applications. *Energy Environ. Sci.* **4**, 398 (2011).
35. Kresse, G. & Furthmüller, J. Efficiency of ab-initio total energy calculations for metals and semiconductors using a plane-wave basis set. *Computational Materials Science* **6**, 15 (1996).

Acknowledgements

We gratefully acknowledge IIT Ropar for providing the High Performance Supercomputing facility and CDAC-Pune for the PARAM YUVA II Supercomputing facility. R. Kumar and Deepika acknowledges P. Wadhwa for her support in data collection during preparation of the manuscript.

Author Contributions

R.K. conceived and supervised the study. D., S.K., A.S. and R.K. developed the model for study. D. carried out the computations. All authors discussed and analyzed the results and co-wrote the paper. All authors reviewed the manuscript.

Additional Information

Supplementary information accompanies this paper at <http://www.nature.com/srep>

Competing financial interests: The authors declare no competing financial interests.

How to cite this article: Deepika *et al.* Origin of multiple band gap values in single width nanoribbons. *Sci. Rep.* **6**, 36168; doi: 10.1038/srep36168 (2016).

Publisher's note: Springer Nature remains neutral with regard to jurisdictional claims in published maps and institutional affiliations.



This work is licensed under a Creative Commons Attribution 4.0 International License. The images or other third party material in this article are included in the article's Creative Commons license, unless indicated otherwise in the credit line; if the material is not included under the Creative Commons license, users will need to obtain permission from the license holder to reproduce the material. To view a copy of this license, visit <http://creativecommons.org/licenses/by/4.0/>

© The Author(s) 2016

SCIENTIFIC REPORTS

OPEN

Erratum: Origin of multiple band gap values in single width nanoribbons

Deepika, Shailesh Kumar, Alok Shukla & Rakesh Kumar

Scientific Reports 6:36168; doi: 10.1038/srep36168; published online 03 November 2016; updated on 30 November 2016

The original version of this Article contained errors in the name of the author Deepika, which was incorrectly given as Deepika Goyal.

These errors have now been corrected in the PDF and HTML versions of the Article.



This work is licensed under a Creative Commons Attribution 4.0 International License. The images or other third party material in this article are included in the article's Creative Commons license, unless indicated otherwise in the credit line; if the material is not included under the Creative Commons license, users will need to obtain permission from the license holder to reproduce the material. To view a copy of this license, visit <http://creativecommons.org/licenses/by/4.0/>

© The Author(s) 2016